

Classification of Lymphocytosis from Blood Cells

Deep Learning for Medical Imaging

Clément Grisi

École des Ponts ParisTech

grixi.clement@gmail.com

Marius Schmidt-Mengin

École des Ponts ParisTech

marius.schmidt.mengin@gmail.com

Abstract

In this report, we emphasize our work for the data challenge organized as part of the Deep Learning for Medical Imaging class. The goal of the challenge is to classify lymphocytosis from blood cells. Through iterations in model definition and data representation, we managed to get 0.96623 classification accuracy on the academic leaderboard (rank 1).

1. Introduction

Lymphocytosis is an increase in the number or proportion of lymphocytes in the blood. It's a common finding, which can be either a reaction to infection or acute stress (reactive), or the manifestation of a lymphoproliferative disorder – a type of cancer of the lymphocytes (tumoral). In clinical practice, the diagnosis as either reactive or tumoral is performed by trained pathologists who visually inspect blood cells under a microscope. The final decision also takes into consideration clinical attributes such as age, gender, and lymphocyte count. In spite of being relatively fast and affordable, lymphocytosis diagnosis lacks reproducibility between experts. Additional clinical tests are often required to confirm the malignant nature of the lymphocytes. However, this analysis is relatively expensive and time-consuming, and therefore is not performed for every patient in practice. In this context, automatic classification has the potential to provide accurate and reproducible diagnosis, saving precious time and resources by quickly identifying which patient should be referred for flow cytometry analysis.

2. Problem Definition

2.1. Dataset

Blood smears and patient attributes were collected from 204 patients from the routine hematology laboratory of the Lyon Sud University Hospital. All included patients have a lymphocyte count above $4 \times 10^9/L$. The blood smears

were automatically produced by a Sysmex automat tool, and the nucleated cells were automatically photographed with a DM-96 device. The training set consists of 142 patients (44 reactive and 98 malignant cases), and the testing set of 42 patients. For each patient, we have access to dozens of images of lymphocytes, as well as the following clinical attributes: gender, age, and lymphocyte count.

2.2. Evaluation Metric

This challenge is evaluated on balanced accuracy (BA), which normalizes true positive (TP) and true negative (TN) predictions by the number of positive and negative samples, respectively. In particular, if one denotes false positives as FP and false negatives as FN, we have:

$$\text{Sensitivity} = \frac{\text{TP}}{\text{TP} + \text{FN}}, \quad \text{Specificity} = \frac{\text{TN}}{\text{TN} + \text{FP}}$$

$$\text{BA} = \frac{\text{Sensitivity} + \text{Specificity}}{2}$$

2.3. Weak Supervision through Multiple Instance Learning

The idea of weakly supervised learning is to exploit coarse-grained annotations to automatically infer finer-grained information. Coarse-grained information is often readily available in the form of patient level labels, but finer grained annotations are more difficult to obtain. Without precise local annotations, classification models cannot be trained in a fully supervised manner. Therefore, various weakly supervised techniques have recently been developed to overcome this issue. One of these techniques relies on multiple instance learning (MIL), an existing framework largely used in classic computer vision that has recently showed state-of-the-art results in several medical imaging tasks [1].

Babenko [2] gives a good example to understand multiple instance learning. Imagine several people, each of them

having a key chain that contains a few keys. Some of these people are able to enter a certain room, and some aren't. The task is to predict whether or not a given key chain can open the door of that room. To solve this problem, one needs to find the exact key that is common to all the *positive* key chains. If one can correctly identify this key, one can also correctly classify an entire key chain - *positive* if it contains the required key, or *negative* if it doesn't.

Hence, the multiple instance learning framework allows the training of a classifier from weakly labeled data: instead of providing input-label pairs, labels ℓ_b are assigned to *sets* or *bags* of instances. In this setting, the true instance labels ℓ_i can be thought of as latent variables, as they are not known during training. In our case, we can assume that only a subset of the images available for a patient with tumoral lymphocytosis do carry the information necessary to correctly classify that patient. Identifying these special instances perfectly fits in the multiple instance learning framework.

3. Methodology

3.1. Standard MIL Assumption

Under the standard MIL assumption, *positive* patients must contain at least one instance classified as *positive*, while *negative* patients, instead, must have all their instances classified as *negative*.

The full pipeline is described on Figure 1. Each forward + backward pass can be broken down into two consecutive stages:

- the *inference* phase: during *inference*, the models' weights are frozen. Each instance is run through the network and assigned a number between 0 and 1: the more likely an instance to indicate tumoral lymphocytosis, the closer the number assigned to 1. Once all the instances of a patient have been processed, they can be ranked according to their probability of being *positive*. For each patient, the top-1 instance is selected for the second stage: the *learning* phase.
- the *learning* phase: we now allow the models' weights to be updated. Given the standard MIL assumption detailed above, one can expect the top-1 instance of a *positive* patient to be *positive*, and the top-1 instance of a *negative* patient to be *negative*. Hence, as we run the top-1 instance through the network, we assign them the label of the patient they come from and update the weights accordingly: the network adjusts its weights in order to assign high probabilities to the top-1 instances coming from positive patients, while keeping low probabilities for the top-1 instances in negative patients.

At this stage, you might be wondering “*how this model converges ?*”. It is true that it is not obvious as the model is initialized with ImageNet pre-trained weights, hence there's not reason to believe the model will assign high probabilities to the true positive instances, and low probabilities to true negative instances. And actually, the model does start by assigning random probabilities to each instances!

To understand how the model gradually learns to discriminate positive instances from negative ones, we need to focus on negative patients, who play a key role in the early stages of training. Under the standard MIL assumption , we know these patients must have all their instances classified as negative. At the end of the first *inference* phase, the model has assigned these instances random probabilities, which can be either high or low. Hence, the top-1 instance for negative patient is random. I claim that this doesn't matter. Let me explain you why. What's important is what happens during the first *learning* phase: for each negative patient, we have a (random) instance, which is negative. The model must adjust its weights to assign lower probabilities to each negative instances, such that at the following *inference* step, all instances that look similar to negative instances will be assigned lower probabilities. As a result, all negative instances start to be assigned low probabilities, and positive instances will strand out, with higher probabilities. At this point, the top-1 instance of a positive patient is more likely to be a true positive. And the model will adjust its weights to assign higher probabilities to this type of instance.

This simplified reasoning allows to understand how the model gently learns to discriminate suspicious instances from non-suspicious ones, and automatically infers fine-grained information from coarse-grained labels.

The standard MIL assumption implies that a patient is classified positive as soon as the model identifies a suspicious instance in its corresponding bag of instances. During testing, if the top-1 instance probability is above the classification threshold τ_{class} , the whole bag is classified positive, otherwise it's classified negative. Letting the top-1 instance decide for the whole bag might be too sensitive. Imagine there exists different degrees of severity among positive instances. Looking only at the top-1 instance will correctly identify the most severe positive instances, but miss the less severe ones, which might be just as important for the final classification.

3.2. Extending the Scope of the Model

In order to deal with the limitation highlighted in the previous section, we came up with two different ideas:

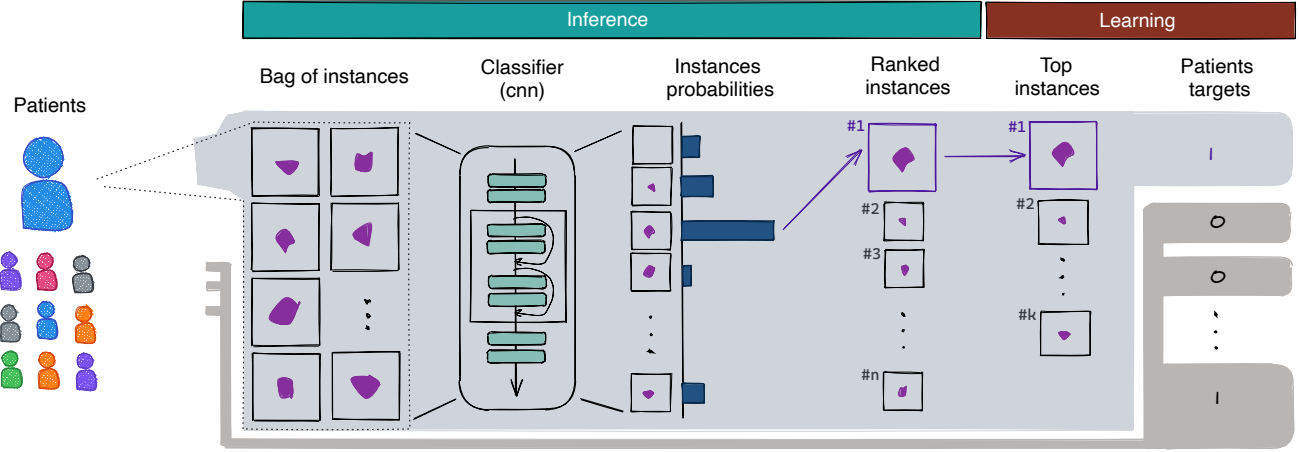


Figure 1: MIL Pipeline

- extend the standard MIL assumption by introducing of a hyperparameter k_{train} which forces the model to look for at least k_{train} positive instances in positive bags, instead of only 1
- still train with top- $k = 1$, but introduce a hyperparameter k_{agg} to control the number of instances to aggregate for the final prediction.

Both ideas extend the scope of the model as we no longer let one instance decide for the label assigned to a patient. When taking more instances into account, one need to come up with a strategy to aggregate their probabilities into a single patient-level probability. As we pointed out in the previous section, applying a *max* over instances' probabilities has the adervse effect of letting the top instance decide for the whole bag. Instead, we might want to consider taking the *mean* probability of the top- k instances. Indeed, there are reason to think that n consecutive instances with high probabilities is a different biomarker than 1 instance with high probability, followed by $n - 1$ instances with probabilities close to zero. Taking the mean probability would allow to distinguish these two cases.

The experiments conducted tend to confirm that the performances of our model were sensitive to the value of both k_{train} and k_{agg} parameters. Using a fixed top- k , however, does not generalize well, since different patients have different numbers of instances, hence different numbers of suspicious instances. In order to account for this, one can introduce percentage-based $k_{\text{train}} - k_{\text{agg}}$ values by looking at

$$\max(m, \lceil k\% \text{ of instances} \rceil)$$

where m is a new hyperparameter that controls the minimum number of instances to aggregate for the final prediction. Given the limited time of the Kaggle challenge, we

didn't implent this idea, but encourage the interested reader to do so.

3.3. Taking More Tiles into Consideration

According to [3], bottom- k instances are the regions “which best support the absence of the class” and could be just as useful as top- k instances to determine the patient label. Indeed, we can expect the bottom- k instances of a positive patient to have a different morphological aspect than that of a negative patient, which could help refining the lymphocytosis diagnosis. Based on these findings, we decided to take the bottom- k probabilities into account as well when deriving a patient’s probability, computing the average probability on the k_{agg} top instances plus the k_{agg} bottom intances.

Results suggest bottom- k instances are just as useful as top- k instances to determine the patient label. Hence, there are reasons to believe that taking all instance into consideration and letting the model identify useful instances for classification could lead to improved results. This is precisely what we investigate in the following section.

3.4. Taking All Instances into Consideration

Instead of only aggregating the model’s output on a subset of instances into a single patient-level quantity, we wanted to design a custom aggregation function that would take all instances into consideration.

3.4.1 Theoretical Overview

Let us denote all the predictions (logits) for patient j by ℓ_i^j , $i = 1 \dots n_j$. To aggregate these predictions, we seek to define some weights $\alpha_i^j \geq 0$ such that we can compute the

final prediction logit for patient j by

$$\ell^j = \sum_{i=1}^{n_j} \alpha_i^j \ell_i^j$$

(we assume that $\sum_i \alpha_i^j = 1$). The confidence score is then given by applying the sigmoid function: $y_j = \sigma(\ell^j)$. Two very common aggregation functions are the arithmetic mean and the maximum, where we would respectively set $\alpha_i^j = 1/n_j$ and

$$\alpha_i^j = \begin{cases} 1 & \text{if } \ell_i^j = \max_k \ell_k^j \\ 0 & \text{otherwise} \end{cases}$$

We believe that these two aggregation function suffer from different problems. Let us express the gradient of the cross-entropy loss with respect to the logits ℓ_i^j :

$$\frac{\partial L_{CE}}{\partial \ell_i^j} = \alpha_i^j (y^j - \bar{y}^j)$$

The maximum function results in sparse gradients (only one α_i^j is nonzero), as only the image that effectively generated the maximum produces a nonzero gradient. On the other hand, the mean function generates equal gradients for all images (all α_i^j are equal to $1/n_j$), meaning that for a positive patients, the "pull" generated by the gradient on negative images (if there are any) is equal to the pull applied to positive images. We developed an aggregation function that intuitively overcomes this problem. The idea behind it is similar to focal loss [4], which scales the weight so as to put more gradient on predictions that are deemed important in the context of a heavy class imbalance. Our aggregation function defines the weights α_i^j by batch normalization [5] followed by the sigmoid function:

$$\alpha_i^j = \sigma \left(\beta + \gamma \frac{\tilde{\ell}_i^j - \mu}{\sqrt{V + \epsilon}} \right)$$

where $\tilde{\cdot}$ denotes the stop gradient operation (as in focal loss, no gradients are propagated through the weights), γ and β are trainable parameters, ϵ is a small constant and μ and V are respectively the mean and variance of the logits ℓ_i^j over a batch of patients:

$$\mu = \frac{1}{n_1 + \dots + n_B} \sum_{j=1}^B \sum_{i=1}^{n_j} \ell_i^j$$

$$V = \frac{1}{n_1 + \dots + n_B} \sum_{j=1}^B \sum_{i=1}^{n_j} (\ell_i^j - \mu)^2$$

where B is the batch size. Intuitively, α_i^j is small when ℓ_i^j is small compared to the rest of the batch, i.e, when it is likely to be a negative sample.

```
logits = conv(features) # 1 channel
weights = bn(logits.detach())
weighted_logits = weights * logits
y = sigmoid(weighted_logits.sum() / weights.sum())
```

Pseudo-code 1: PyTorch-like pseudo-code for our custom aggregation function

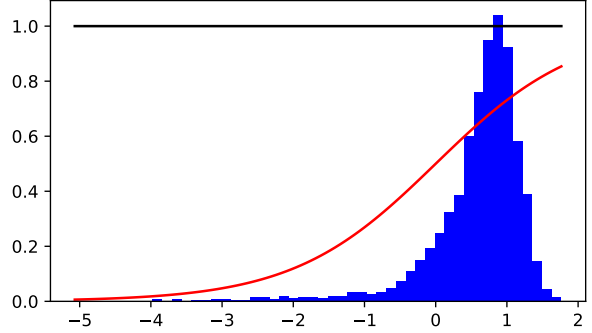


Figure 2: The distribution of the batch normalized logits over a bag is shown in blue. The red sigmoid shows the weight that is associated to each logit. The smaller the logit, the smaller the weight.

3.4.2 Practical Implementation

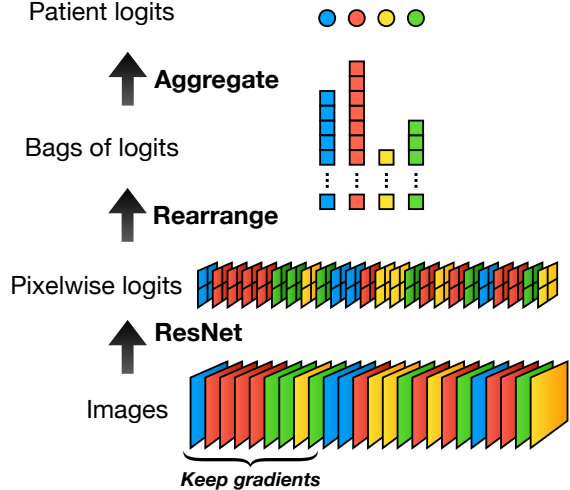


Figure 3: Baseline architecture.

We adopt a simple and explainable architecture composed of a ResNet [6] backbone followed by an aggregation module. For a given batch of patients, we take all their images and stack them into a batch. This batch is passed independently the backbone, without global pooling. A 1×1 convolution with one output channel is then applied to the resulting feature maps to obtain pixelwise prediction logits. These logits are rearranged into bags of scores, each

bag corresponding to all prediction for one patient. Finally, the aggregation module transforms each bag of scores into a final patient prediction.

It is common that the features are aggregated before being linearly mapped to the final prediction score. In contrast, we apply the aggregation after reducing each feature to a single prediction logit. We did not find this to impact the results (and in the case where the aggregation function is linear, both methods are equivalent). Doing so makes the model more interpretable as each pixel (in the feature space) of each image can be given a score.

As the number of images passed through the backbone is often large, we keep the gradients for only a random subset of these images. Pseudo-code for this is provided by Algorithm 1.

```
B, 3, H, W = image_batch.shape
max_forward_size = 512
max_backward_size = 512
features = []
i = 0
# forward images without keeping gradients
with torch.no_grad():
    while i < B - max_backward_size:
        j = min(i+max_forward_size,
                 num_images-max_backward_size)
        features.append(backbone(images[i:j]))
        i = j
# forward image with gradients
features.append(backbone(images[i:j]))
# Note: the images are supposed
# so that the subset for which
# are kept is random.
```

Pseudo-code 2: PyTorch-like pseudo-code for propagating the gradients through only a subset of the images, in order to not run out of GPU memory.

4. Results

We start with the simple model that only looks at the top-1 instance, then we evaluate how the different ideas successively described in Section 3 impact our performances. The ablation study is solely conducted for the custom aggregation function we designed, as it ended up outperforming all other approaches by a significant margin.

To compare the different methods fairly, we always run 10 different trainings. Each training has its own seed for initializing the model and splitting the dataset (50/50 split). The 10 seeds are kept the same for each configuration. Each model is trained for 40 epochs with a batch size of 16, resulting in 5 batches per epoch. Evaluation if

performed at the end of every epoch. We always optimize with Adam and a learning rate of 10^{-4} . When we report a metric for any configuration, we average the 10 best values of each training, and again average this over all 10 trainings (the average is thus taken over 100 values). We always report 95% confidence intervals.

4.1. Augmentations

As the images are centered on a lymphocytes, we always apply a center crop of size 112 to all images (training, validation and testing). Initial experiments showed that this significantly improves the accuracy and reduces the computational resources. We use vertical and horizontal random flipping. We tried to use more aggressive augmentations such as affine transforms and color jittering but this heavily impaired the accuracy.

4.2. Backbone Choice

We compared three backbones: ResNet18, ResNet34 and ResNet50 [6]. We also tried a more recent backbone, EfficientNet [7], but did not obtain good results. Results for the custom aggregation are summarized in Figure 4. ResNet18 achieves the best validation balanced accuracy. This is also what we observe for other aggregation functions. We use ResNet18 for all our subsequent experiments.

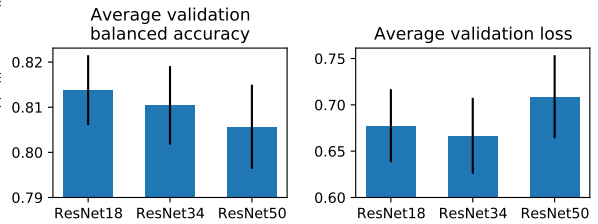


Figure 4: Impact of ResNet depth on validation loss and balanced accuracy. The black bars indicate 95% confidence intervals. Shallower seems to be better but the results are not very significative.

4.3. Working on a Subset of Instances

add top-1, top- k , top- k and bottom- k results

4.4. Working on a All Instances

4.5. Number of images

In the previous sections, when doing one training step, we used all the images of each patient and aggregated their logits. In this experiment, we use only a small random subset of image per patient during each training step. We posit that selecting only a small subset of images provides some regularization to the training process. Indeed, assume that for a given positive patient, one image is easily

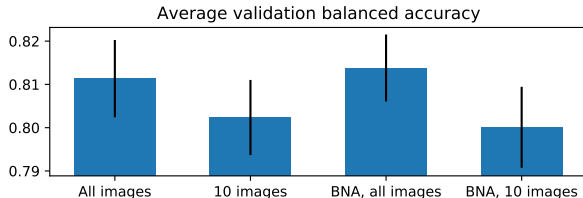


Figure 5: The performance when training with subsets of 10 images was generally worse.

identified by the network as positive. In this case, the network can ignore the other images. By selecting only a small random subset of images, we avoid this problem, as the easy positive image has a high probability of not being selected. Note that we implicitly make the assumption that in the case of a positive patient, a large number of images contains positive information. This idea is similar to hard negative mining, and could be called “easy positive avoidance”.

Our winning submission was obtained with this strategy but Figure 5 shows that it actually worsened the results when evaluated over 10 runs¹.

5. Explainability

Multiple instance learning is very handy as it provides different ways to visualize what the model learned. This is of an inestimable value as deep learning models are often criticized for their lack of explainability. They are frequently referred to as *black boxes* in the sense that one can’t really inspect how they end up predicting one thing instead of another. Summarizing what is discussed in Sections 3.1 to 3.3, the final classification of a patient is the result of several consecutive steps:

- an inference step mapping each input instance to a probability
- a ranking step sorting instances by decreasing probability
- a learning step comparing the k_{train} instances probabilities patient labels to update the model’s weights
- an aggregation step combining k_{agg} probabilities into a single prediction

Keeping track of instances probabilities allows deep inspection of the workings of our models. Indeed, comparing instances our model identifies positive with those it identifies negative can reveal which visual patterns the model uses to

¹When training with 10 images per patient per batch, we trained for 120 epochs instead of 40, but performed evaluation only every third epoch (so that the number of evaluations is kept the same).

discriminate between reactive and tumoral lymphocytosis. For lack of time, we didn’t conduct this analysis.

6. Conclusion

Future work: dilated ResNet ?

Future work: aggregate embeddings using a recurrent neural network / self-attention encoder?

References

- [1] Le Hou, Dimitris Samaras, Tahsin M. Kurç, Yi Gao, James E. Davis, and Joel H. Saltz. Efficient multiple instance convolutional neural networks for gigapixel resolution image classification. *CoRR*, abs/1504.07947, 2015. [1](#)
- [2] Boris Babenko. Multiple instance learning: algorithms and applications. 2008. [1](#)
- [3] Charlie et al. Saillard. Predicting survival after hepatocellular carcinoma resection using deep learning on histological slides. *Hepatology*, 72, 02 2020. [3](#)
- [4] Tsung-Yi Lin, Priya Goyal, Ross B. Girshick, Kaiming He, and Piotr Dollár. Focal loss for dense object detection. In *IEEE International Conference on Computer Vision, ICCV 2017, Venice, Italy, October 22-29, 2017*, pages 2999–3007. IEEE Computer Society, 2017. [4](#)
- [5] Sergey Ioffe and Christian Szegedy. Batch normalization: Accelerating deep network training by reducing internal covariate shift. In Francis R. Bach and David M. Blei, editors, *Proceedings of the 32nd International Conference on Machine Learning, ICML 2015, Lille, France, 6-11 July 2015*, volume 37 of *JMLR Workshop and Conference Proceedings*, pages 448–456. JMLR.org, 2015. [4](#)
- [6] Kaiming He, Xiangyu Zhang, Shaoqing Ren, and Jian Sun. Deep residual learning for image recognition. *CoRR*, abs/1512.03385, 2015. [4, 5](#)
- [7] Mingxing Tan and Quoc V. Le. Efficientnet: Rethinking model scaling for convolutional neural networks. In Kamalika Chaudhuri and Ruslan Salakhutdinov, editors, *Proceedings of the 36th International Conference on Machine Learning, ICML 2019, 9-15 June 2019, Long Beach, California, USA*, volume 97 of *Proceedings of Machine Learning Research*, pages 6105–6114. PMLR, 2019. [5](#)

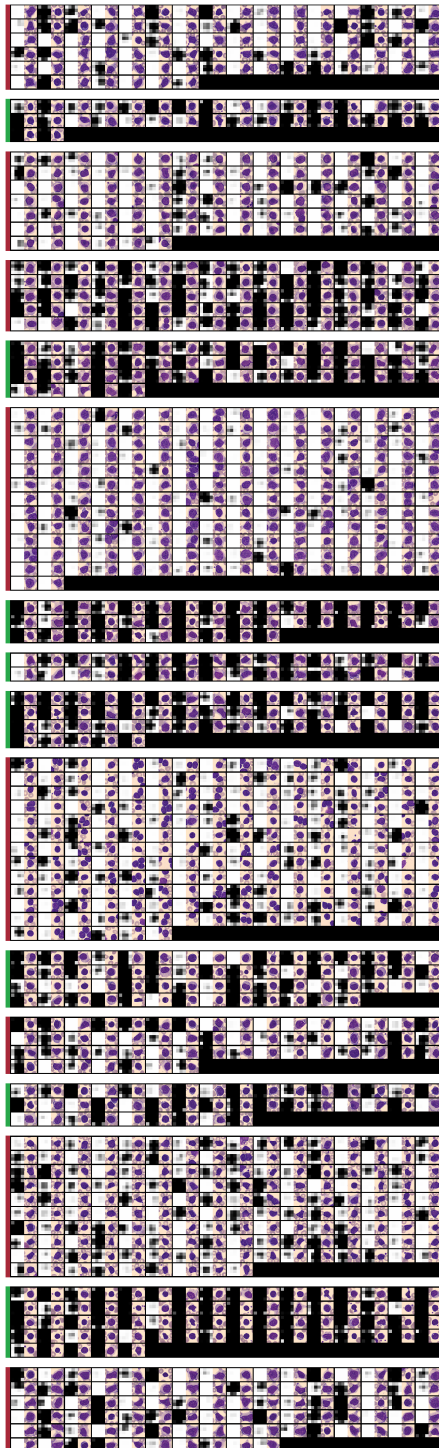


Figure 6: Predictions and images for 16 patients from the validation set. The patients were not cherry-picked. For each patient, a red left border indicates a positive ground truth label while green indicates a negative one. For each lymphocyte image, we provide on the left the 4×4 predictions of the network. White means a score of one and black a score of 0.